Biochemistry

Article

pubs.acs.org/biochemistry

Sugars Require Rigid Multivalent Displays for Activation of Mouse Sperm Acrosomal Exocytosis

He Huang, Maria T. Rodolis, Surita R. Bhatia, and Nicole S. Sampson*

Department of Chemistry, Stony Brook University, Stony Brook, New York 11794-3400, United States

Supporting Information

ABSTRACT: As a prerequisite to mammalian fertilization, the sperm acrosomal vesicle fuses with the plasma membrane and the acrosome contents are exocytosed. Induction occurs through engagement of the sperm receptors by multiple sugar residues. Multivalent polymers displaying mannose, fucose, or GlcNAc are effective synthetic inducers of mouse sperm acrosomal exocytosis (AE). Each carbohydrate is proposed to have a distinct binding site on the sperm cell surface. To determine the role of the scaffold structure in the efficiency of AE induction, different polymer backbones were employed to display the different activating sugar residues. These glycopolymers were prepared by ruthenium-catalyzed ring-opening metathesis of 5-substituted norbornene or cyclooctene. The conformations of the glycopolymers were characterized by small-angle X-ray scattering. Polynorbornene displaying mannose, fucose, or GlcNAc forms flexible cylinders in aqueous solution. However, polycyclooctenes displaying any of these same sugars are much more flexible and form random coils. The flexible polycyclooctenes displaying fucose or GlcNAc were less effective inducers of AE than their norbornene counterparts. In contrast, polycyclooctene displaying mannose was the most effective AE inducer and had a more collapsed spherelike structure. Our results suggest that the AE efficacy of fucose, GlcNAc, and mannose polymers relies on a relatively rigid polymer that can stabilize receptor signaling complexes.

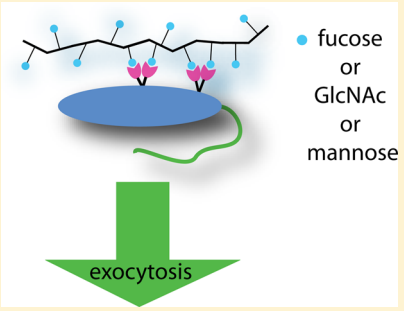

Carbohydrate−protein interactions are involved in a wide variety of biological processes, including fertilization[2−4] and implantation,[5] pathogen invasion,[6] immune response,[7,8] and cell growth regulation.[9] Despite weak affinities of individual carbohydrate−protein interactions, multivalent glycoconjugates, such as glycopolymers, glycodendrimers, and glyconanoparticles, with multiple carbohydrate ligands can enhance overall binding avidity.[10,11]

Synthetic glycopolymers provide access to a large variety of overall structures and are popular multivalent glycoconjugates because of their ease of synthesis. Different polymerization strategies provide varying polymer backbone rigidities as well as binding group spacing and density.[10] The flexibility of the polymer scaffold is one of the factors that can affect the biological activity of the glycoconjugate.[12] A rigid polymer with correct spacing may interact with receptors more exactly to avoid a conformational entropy penalty.[10] Alternatively, flexible polymers are more capable of adapting to protein interfaces and of clustering more carbohydrate-binding proteins.[13,14] Therefore, the effect of the polymer backbone flexibility depends on the receptors engaged and their presented orientations on the backbone.[15]

We are interested in how polymer backbones affect induction of mouse sperm acrosomal exocytosis (AE) by glycopolymers. AE is a key step in mammalian fertilization, and only sperm that have undergone AE can participate in the subsequent fertilization steps that lead to sperm−egg fusion.[16] Previous studies by our group[17] and others[18] found that polynorbornene glycopolymers displaying mannose, fucose, or GlcNAc or a protein displaying mannose, GlcNAc, or GalNAc can initiate AE *in vitro*. However, the identity of the sperm receptors remains unknown.

Here, we compare these inducers of AE to glycopolymers displaying the same sugars on a different backbone, polycyclooctene (Figure 1). Both polymers are prepared through ruthenium-catalyzed ring-opening metathesis polymerization (ROMP). Polynorbornene backbones are widely adopted during polymer synthesis because of the high ring strain of norbornene and the high polymer rigidity that results

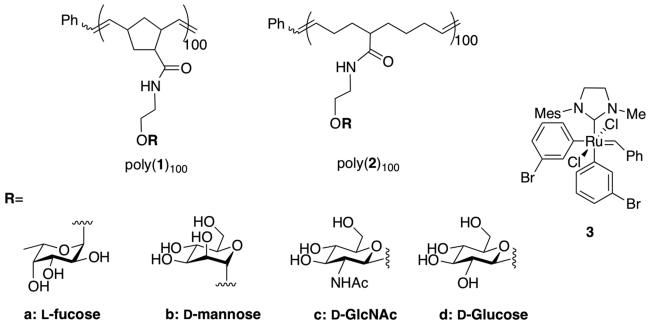

Figure 1. Norbornene poly(**1**)$_{100}$ and cyclooctene poly(**2**)$_{100}$ backbone polymer structures.

Received: February 22, 2017
Revised: May 12, 2017
Published: May 16, 2017

DOI: 10.1021/acs.biochem.7b00166
Biochemistry 2017, 56, 2779−2786

from a cyclopentane in the backbone.[19,20] Functionalized polycyclooctenes are of interest because the backbone can provide a longer interligand spacing along a flexible, acyclic backbone.[21] AE induction activity may be enhanced when the spacing between two ligands is increased, making the binding site more accessible. Moreover, polycyclooctenes are of interest because multiple positions can be substituted with different functional groups on the cyclooctene (COE) backbone.[22] Comparison of the polymer structures by small-angle X-ray scattering (SAXS) in the solution state and their activity as inducers of AE revealed that the polynorbornene backbone with a rigid cylindrical structure forms more effective inducers of AE when fucose or GlcNAc is presented and the flexible polycyclooctene forms a more effected AE inducer when mannose is presented. Our results demonstrate that activation of AE is dependent on the scaffold structure as well as the pendant sugars.

MATERIALS AND METHODS

Materials. Unless otherwise noted, all reagents were used as supplied by commercial suppliers without further purification. $(H_2IMes)(3\text{-}BrPyr)_2Cl_2Ru{=}CHPh$ (**3**) was prepared according to the method described in the literature.[23] CH_2Cl_2, benzene, Et_2O, tetrahydrofuran (THF), and CH_3OH were dried in a GlassContour solvent pushstill system; pentane was used without further purification. All reactions were performed under an Ar atmosphere in oven-dried glassware unless otherwise specified. Analytical thin layer chromatography (TLC) was performed with precoated silica gel plates (60F254); flash chromatography was performed with silica gel-60 (230−400 mesh), and Combi-Flash chromatography was performed with RediSep normal phase silica columns (Teledyne Isco, silica gel-60, 230−400 mesh). Bruker 400 and Bruker 500 MHz nuclear magnetic resonance (NMR) instruments were used to perform NMR analyses. ^{1}H NMR spectra are reported as chemical shift in parts per million (multiplicity, coupling constant in hertz, integration) and were acquired in $CDCl_3$ unless otherwise noted. ^{1}H NMR data are assumed to be first-order.

Methods. For the determination of $Đ_m$ (dispersity index), polymers (before flash column chromatography purification) were dissolved in $CDCl_3$ (0.5 mg/mL). An aliquot (100 μL) of the polymer solution was injected and analyzed by gel permeation chromatography using a Phenogel column (300 mm × 7.80 mm, 5 μm, linear mixed bed, 0−40K molecular weight range). Elution was performed at a rate of 0.7 mL/min with THF and detection at 220 and 254 nm at 30 °C. Narrowly dispersed polystyrene standards from Aldrich were used as molecular weight calibrants. The number-average and weight-average molecular weights were calculated from the chromatogram.

Poly(1)$_{100}$ Preparation. The norbornene mannose, fucose, GlcNAc, and glucose monomers were synthesized as described by Wu and Sampson.[17]

4-Cyclooctenecarboxylic Acid. 5-Bromo-1-cyclooctene was prepared according to the procedure described by Ashby and Coleman.[24] The 5-bromo-1-cyclooctene was converted to the nitrile using the method described by Hillmyer et al.[21] Hydrolysis of nitrile was performed on the basis of the procedure of Hartley for the preparation of δ-oxoazelaic acid.[25] Specifically, 1.3 mL of 30% (v/v) H_2O_2 was added to a suspension of 6.1 g of nitrile and 20.2 mL of 30% (w/v) aqueous KOH. The mixture was stirred under N_2 and heated at 40 °C for 1 h, after which it was heated at reflux for 20 h. The mixture was cooled to room temperature and extracted with Et_2O to remove traces of the starting material. The aqueous phase was acidified with 20 mL of a 40% (v/v) aqueous solution of phosphoric acid and stirred for 2 h. The aqueous solution was then extracted with Et_2O (3 × 50 mL), and the Et_2O was dried over Na_2SO_4 and concentrated in vacuo to obtain 1.2 g of the title acid (49% overall yield): ^{1}H NMR ($CDCl_3$) δ 13.4−9.7 (1H, bs), 5.72−5.60 (2H, m), 2.50 (1H, m), 2.40 (1H, m), 2.25−2.03 (4H, m), 1.90 (1H, m), 1.73 (1H, m), 1.65 (2H, m), 1.40 (1H, m).

Cyclooctene Monomers (2). Azido L-fucose, D-mannose, D-*N*-acetylglucosamine, and D-glucose sugar monomers were synthesized and coupled to 4-cyclooctenecarboxylic acid as described by Wu and Sampson.[17] Monomer **2a′** was purified by chromatography [1:1 (v/v) EtOAc/CH_2Cl_2 (Combi-Flash)]. Monomer **2b′** and monomer **2d′** were purified by chromatography [1:3 (v/v) EtOAc/CH_2Cl_2 (Combi-Flash)]. Monomer **2c′** was purified by chromatography [EtOAc (Combi-Flash)]. Monomers **2a′**, **2b′**, **2c′**, and **2d′** were obtained in 65, 75, 75, and 85% yields, respectively.

2a′: ^{1}H NMR (CD_2Cl_2, 500 MHz) δ 7.78 (d, J = 8.4 Hz, 1H), 7.63 (dd, J = 24.2, 8.0 Hz, 1H), 7.41−7.21 (m, 2H), 6.05−5.92 (m, 1H), 5.64−5.45 (m, 2H), 5.28−5.10 (m, 2H), 5.06−4.88 (m, 3H), 4.79 (t, J = 5.4 Hz, 1H), 4.09−3.95 (m, 1H), 3.80−3.58 (m, 3H), 3.45−3.23 (m, 3H), 2.34−2.21 (m, 1H), 2.18−1.89 (m, 12H), 1.88 (s, 3H), 1.85−1.72 (m, 2H), 1.70−1.45 (m, 5H), 1.34−1.08 (m, 3H), 1.01 (dd, J = 21.4, 6.5 Hz, 14H); ^{13}C NMR ($CDCl_3$, 126 MHz) δ 178.0, 170.8, 170.4, 130.9, 130.8, 129.8, 96.6, 77.5, 77.4, 77.2, 71.3, 71.2, 71.1, 70.3, 68.30, 68.07, 67.96, 67.79, 67.76, 65.01, 64.80, 45.7, 42.3, 39.1, 32.7, 30.5, 29.8, 28.3, 26.18, 26.1, 24.3, 23.7, 21.0, 20.9, 20.8, 16.0, 1.2.

2b′: ^{1}H NMR ($CDCl_3$, 500 MHz) δ 5.90 (q, J = 5.9 Hz, 1H), 5.63 (dtd, J = 19.9, 10.8, 9.9, 3.8 Hz, 2H), 5.30−5.17 (m, 3H), 4.76 (s, 1H), 4.21 (dd, J = 12.3, 5.6 Hz, 1H), 4.10−4.00 (m, 1H), 3.90 (t, J = 7.7 Hz, 1H), 3.86−3.66 (m, 1H), 3.47 (tt, J = 8.1, 3.6 Hz, 2H), 3.39−3.29 (m, 1H), 2.34 (dtt, J = 14.1, 8.9, 4.4 Hz, 1H), 2.21 (dp, J = 12.5, 6.5, 6.0 Hz, 1H), 2.18−1.80 (m, 18H), 1.63 (ddt, J = 38.7, 15.2, 6.9 Hz, 5H), 1.35 (tt, J = 15.3, 6.1 Hz, 1H), 1.20 (t, J = 7.1 Hz, 1H), 1.07 (d, J = 6.5 Hz, 2H); ^{13}C NMR ($CDCl_3$, 126 MHz) δ 178.1, 171.2, 170.7, 170.1, 169.7, 157.2, 130.7, 129.8, 97.7, 77.5, 77.4, 77.2, 69.4, 69.1, 68.7, 67.4, 66.2, 62.5, 60.5, 45.5, 42.0, 38.9, 32.7, 32.5, 30.5, 30.3, 28.1, 26.0, 24.2, 23.6, 20.9, 20.8, 20.7, 14.2, 1.1.

2c′: ^{1}H NMR ($CDCl_3$, 500 MHz) δ 7.77 (dd, J = 73.8, 8.3 Hz, 1H), 7.40 (dt, J = 26.6, 7.3 Hz, 1H), 6.49 (dd, J = 19.2, 8.4 Hz, 1H), 6.23 (dt, J = 32.0, 6.6 Hz, 1H), 5.73−5.51 (m, 3H), 5.17 (t, J = 10.0 Hz, 1H), 5.04 (q, J = 9.7 Hz, 2H), 4.85−4.73 (m, 0H), 4.61 (t, J = 8.2 Hz, 1H), 4.31 (td, J = 10.0, 3.6 Hz, 0H), 4.20 (ddd, J = 17.5, 12.3, 4.8 Hz, 1H), 4.08 (dd, J = 19.1, 12.5 Hz, 2H), 3.94 (ddt, J = 18.7, 9.5, 4.6 Hz, 1H), 3.80 (q, J = 9.3, 8.1 Hz, 1H), 3.73−3.59 (m, 2H), 3.59−3.37 (m, 2H), 3.30 (qd, J = 13.3, 11.4, 6.2 Hz, 1H), 2.33 (ddt, J = 14.6, 9.7, 5.4 Hz, 1H), 2.23 (q, J = 8.0, 7.5 Hz, 2H), 2.11 (p, J = 6.6 Hz, 3H), 2.05 (d, J = 4.8 Hz, 6H), 1.98 (dd, J = 10.9, 4.2 Hz, 10H), 1.93 (s, 3H), 1.83 (dq, J = 13.6, 4.4 Hz, 1H), 1.74−1.52 (m, 6H), 1.42−1.12 (m, 6H), 1.11−1.01 (m, 1H), 0.82 (dp, J = 26.5, 6.8 Hz, 2H); ^{13}C NMR ($CDCl_3$, 126 MHz) δ 178.7, 171.9, 169.4, 130.6, 129.6, 129.5, 128.4, 126.7, 125.7, 117.9, 110.8, 101.0, 97.8, 77.4, 77.3, 77.1, 72.6, 71.9, 71.3, 68.4, 68.1, 67.8, 62.1, 54.3, 51.6, 45.5, 45.3, 42.2, 39.0, 32.5, 30.4, 30.3, 30.2, 29.7,

DOI: 10.1021/acs.biochem.7b00166
Biochemistry 2017, 56, 2779−2786

29.3, 28.0, 25.9, 24.1, 23.4, 23.0, 22.7, 20.7, 20.6, 19.4, 18.9, 14.1, 5.5.

2d′: ^{1}H NMR ($CDCl_3$, 500 MHz) δ 5.87 (q, J = 5.1 Hz, 1H), 5.60 (dq, J = 31.0, 9.0 Hz, 2H), 5.14 (t, J = 9.5 Hz, 1H), 4.96 (dt, J = 44.2, 9.4 Hz, 2H), 4.58 (d, J = 7.9 Hz, 1H), 4.46 (d, J = 7.9 Hz, 1H), 4.20 (dd, J = 12.4, 4.9 Hz, 1H), 4.11−3.96 (m, 2H), 3.78 (qd, J = 11.9, 10.1, 6.1 Hz, 2H), 3.64 (dddd, J = 19.6, 14.5, 10.1, 5.4 Hz, 2H), 3.36 (dtt, J = 16.8, 11.4, 6.6 Hz, 2H), 2.32 (dtd, J = 14.4, 9.2, 5.0 Hz, 1H), 2.22−1.79 (m, 19H), 1.72−1.51 (m, 4H), 1.31 (tq, J = 13.4, 6.3 Hz, 1H), 1.19 (t, J = 7.0 Hz, 1H), 1.05 (d, J = 6.5 Hz, 4H); ^{13}C NMR ($CDCl_3$, 125 MHz) δ 178.0, 171.2, 170.6, 170.2, 169.5, 157.3, 130.6, 129.7, 100.9, 95.9, 77.5, 77.4, 77.2, 72.7, 71.9, 71.4, 70.7, 69.2, 68.7, 68.3, 67.6, 67.4, 61.9, 60.4, 45.5, 41.8, 39.0, 32.5, 30.4, 30.3, 28.1, 26.0, 24.2, 23.6, 21.0, 20.8, 20.7, 20.6, 20.3, 14.2, 1.0.

General Procedure for Poly(2′) Preparation. Monomer **2′**, catalyst **3**, and solvent were thoroughly dried before being used. Monomer **2′** (100 equiv) and catalyst **3** (1 equiv) were mixed in CH_2Cl_2 to achieve a final monomer concentration of 57 mM and allowed to react at room temperature. The reaction was monitored by TLC and upon completion immediately quenched with ethyl vinyl ether. Typical reaction times were 15−20 min. Polymers were purified by column chromatography to yield poly(**2a′**)$_{100}$, poly(**2b′**)$_{100}$, poly(**2c′**)$_{100}$, and poly(**2d′**)$_{100}$ in 31, 77, 44, and 61% yields, respectively. The protected glycopolymers were analyzed by GPC to determine dispersities (Table 1).

Table 1. Dispersities of Poly(2′)$_{100}$

polymer	M_n^{theor}	M_n [a]	M_w [a]	$Đ_M$ [a]
poly(**2a′**)$_{100}$	46997	68495	77352	1.13
poly(**2b′**)$_{100}$	52797	43094	53202	1.24
poly(**2c′**)$_{100}$	52697	59649	68235	1.14
poly(**2d′**)$_{100}$	52797	35324	47892	1.36

[a]Determined from GPC utilizing a differential refractometer and a multiangle light scattering detector.

Poly(**2a′**)$_{100}$: ^{1}H NMR ($CDCl_3$, 400 MHz) δ 5.57−5.21 (m), 5.14 (d, J = 10.7 Hz), 5.04 (s), 4.12 (d, J = 8.0 Hz), 3.93−3.23 (m), 2.77−2.46 (m), 2.16 (s), 2.06 (s), 1.77−1.16 (m), 1.14 (d, J = 6.4 Hz), 0.96−0.68 (m).

Poly(**2b′**)$_{100}$: ^{1}H NMR (CD_2Cl_2, 500 MHz) δ 6.25−5.70 (br), 5.30 (q, J = 10.6 Hz), 5.22 (s), 5.12 (t, J = 9.5 Hz), 4.96 (t, J = 9.0 Hz), 4.83 (dt, J = 18.6, 9.2 Hz), 4.49 (t, J = 8.2 Hz), 4.15 (dq, J = 12.7, 7.3, 6.0 Hz), 4.04 (dq, J = 12.7, 7.4, 6.9 Hz), 3.75 (dd, J = 9.8, 5.0 Hz), 3.69−3.54 (m), 3.34 (dtd, J = 18.3, 13.3, 7.0 Hz), 2.04 (dd, J = 23.0, 10.2 Hz), 1.97 (s), 1.91 (d, J = 14.1 Hz), 1.64−1.15 (m), 0.79 (q, J = 12.7, 9.6 Hz).

Poly(**2c′**)$_{100}$: ^{1}H NMR ($CDCl_3$, 500 MHz) δ 6.00 (t, J = 5.6 Hz), 5.93−5.76 (m), 5.65 (dddd, J = 22.8, 16.2, 8.6, 4.3 Hz), 5.23−5.11 (m), 5.07 (td, J = 9.7, 6.7 Hz), 4.59 (dd, J = 10.2, 8.2 Hz), 4.22 (ddd, J = 20.7, 12.3, 4.8 Hz), 4.16−4.04 (m), 3.95 (dtt, J = 15.4, 7.3, 3.6 Hz), 3.83 (tdd, J = 9.7, 6.4, 3.4 Hz), 3.66 (ddtt, J = 16.9, 13.4, 7.2, 3.4 Hz), 3.52 (dddt, J = 27.4, 14.1, 6.3, 3.6 Hz), 3.33 (ddddd, J = 22.3, 18.2, 11.5, 7.5, 4.4 Hz), 2.48−2.30 (m), 2.30−2.20 (m), 2.15 (d, J = 7.9 Hz), 2.08 (d, J = 3.6 Hz), 2.05−1.99 (m), 1.98 (s), 1.95 (s), 1.89 (td, J = 10.7, 5.5 Hz), 1.79−1.55 (m), 1.45−1.29 (m), 1.24 (d, J = 2.4 Hz).

Poly(**2d′**)$_{100}$: ^{1}H NMR (CD_2Cl_2, 500 MHz) δ 5.38−5.10 (m), 4.74 (t, J = 5.0 Hz), 4.16 (dq, J = 9.2, 5.2, 3.7 Hz), 3.99 (d, J = 12.4 Hz), 3.94−3.86 (m), 3.71 (tt, J = 10.1, 5.3 Hz), 3.56−3.25 (m), 2.18−1.85 (m), 1.64−1.41 (m), 1.42−1.07 (m).

General Procedure for the Preparation of Poly(2)$_{100}$. Poly(**2′**)$_{100}$ glycopolymers were deprotected under basic conditions and quenched with aqueous HCl following the procedure described by Wu and Sampson.[17] Deprotection was achieved in 30−40% yields.

Poly(**2a**)$_{100}$: ^{1}H NMR (D_2O, 500 MHz) δ 5.46 (s), 4.92−4.73 (m), 4.01 (s), 3.85−3.75 (m), 3.74−3.37 (m), 2.31 (s), 2.25−2.01 (m), 1.66−1.21 (m), 1.11 (s).

Poly(**2b**)$_{100}$: ^{1}H NMR (D_2O, 500 MHz) δ 5.64 (s), 5.38 (s), 5.22 (d, J = 11.7 Hz), 4.96−4.89 (m), 4.71−4.64 (m), 4.11−4.07 (m), 3.79 (s), 3.71−3.58 (m), 3.54 (s), 3.40 (s), 2.74−2.67 (m), 2.66−2.58 (m), 2.40−2.26 (m), 2.17−1.98 (m), 1.98−1.83 (m), 1.68−1.55 (m), 1.38−0.97 (m).

Poly(**2c**)$_{100}$: ^{1}H NMR (D_2O, 500 MHz) δ 5.81−5.71 (m), 5.45 (s), 5.20−4.60 (m), 4.57−4.51 (m), 3.95−3.64 (m), 3.56−3.29 (m), 2.43−2.36 (m), 2.24−1.92 (m), 1.79−1.56 (m), 1.46−1.21 (m).

Poly(**2d**)$_{100}$: ^{1}H NMR (D_2O, 500 MHz) δ 5.41−5.34 (m), 4.89−4.82 (m), 4.77 (d, J = 18.9 Hz), 4.38 (dd, J = 7.4, 3.2 Hz), 3.87 (dd, J = 28.5, 10.5 Hz), 3.77−3.55 (m), 3.37 (dtd, J = 53.2, 20.6, 18.8, 9.5 Hz), 3.20 (t, J = 8.6 Hz), 2.24 (d, J = 14.4 Hz), 1.95 (s), 1.56 (s), 1.41 (s), 1.27 (s).

Small-Angle X-ray Scattering (SAXS). Small-angle X-ray scattering (SAXS) measurements were taken on a Bruker Nanostar U instrument in the high-resolution configuration (Brookhaven National Laboratory, Upton, NY). The wavelength of the beam is 0.15418 nm with a Cu rotating anode source. The nominal distance from sample to detector (Vantec 2000 area detector) was 1.1 m, and the actual distance was calibrated with silver behenate before the measurements. Deprotected glycopolymer solutions were prepared at the indicated concentrations and loaded into quartz capillaries (diameter of 0.1 mm). The capillary was fixed in the sample holder, and scattering data for each sample were collected for 18 h. SAXS data were analyzed using the SasView small-angle scattering analysis software package (http://www.sasview.org/).

Sperm Flow Cytometry Assay and Statistical Analysis. Mouse sperm isolation and flow cytometry experiments were conducted following previously published methods.[1] The acrosome integrity of live sperm was normalized to PBS (negative control) and 5 μM A23187 (positive control). Normalized AE% was calculated using [(AE% of glycopolymer − AE% of negative control)/(AE% of positive control − AE% negative control)]. %AE induced by each polymer concentration was compared with that of the negative control PBS-treated sperm (normalized 0%) and its significance tested with a one-sample t test. The significance of AE% changes between two consecutive concentrations of polymer was tested with a two-sample t test. Statistical tests were performed with R.[26]

RESULTS AND DISCUSSION

Preparation of Poly(2′)$_{100}$. Cyclooctene functionalized at carbon 5 with a sugar moiety proved to be very reactive in ROMP; 100% conversion was achieved in 15−20 min with 0.5 M catalyst at room temperature. Extending the reaction time beyond 20 min resulted in backbiting and the formation of shorter polymers. The dispersities were determined by GPC, and the results are summarized in Table 1.

Comparison of Polymer Backbones as Inducers of Mouse Sperm Acrosome Exocytosis. Our previous studies demonstrated that polynorbornene backbone polymers with fucose, mannose, and GlcNAc ligands activated mouse AE

DOI: 10.1021/acs.biochem.7b00166
Biochemistry 2017, 56, 2779−2786

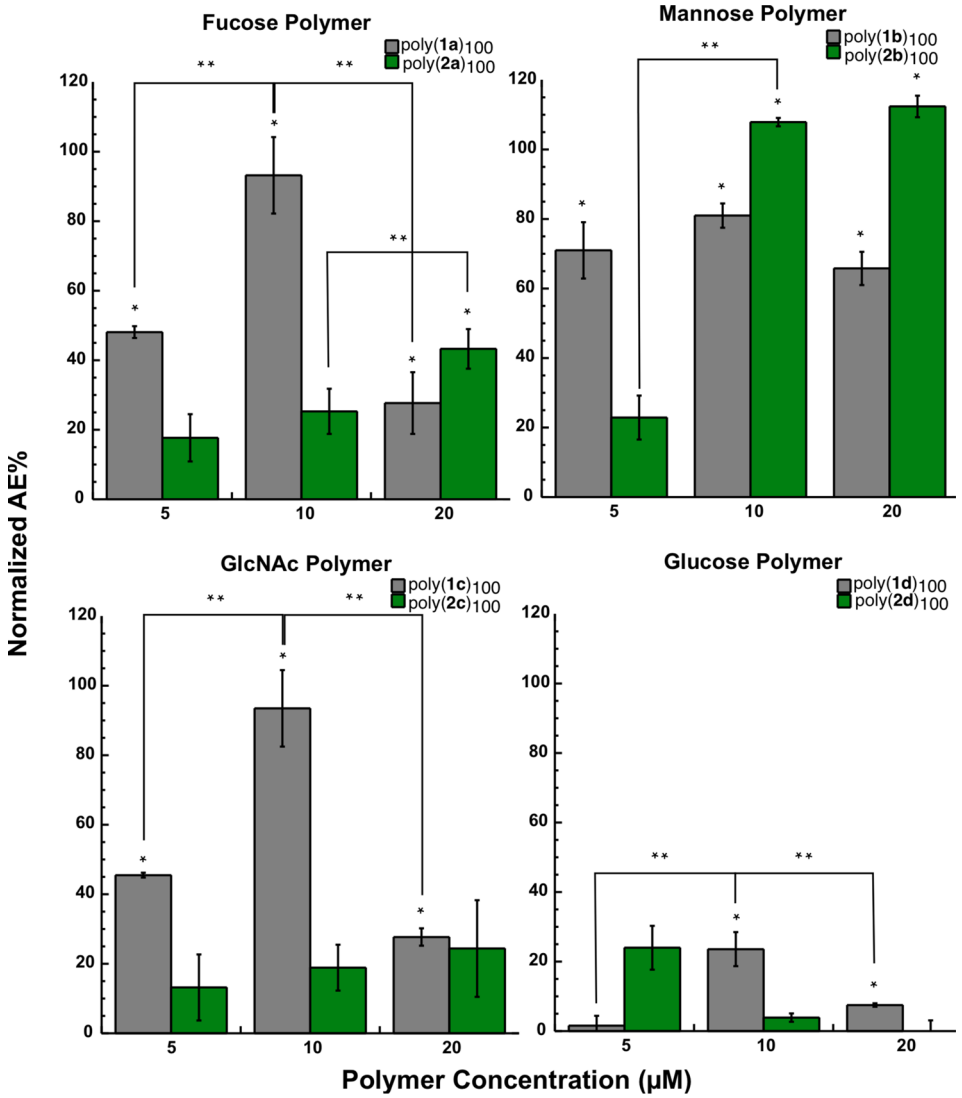

Figure 2. AE induction by norbornene [poly(**1**)$_{100}$][1] and cyclooctene [poly(**2**)$_{100}$] backbone polymers. Normalized AE% = (AE% induction by polymers − AE% induction by negative control)/(AE% induction by positive control − AE% induction by negative control). The average AE% for sperm treated with 5 μM A23187 (positive control) was 21%. The average AE% for sperm treated with PBS (negative control) was 9%. Data represent means ± the standard error of the mean of at least three independent experiments. *p < 0.05 when compared to the negative control. **p < 0.05 when consecutive concentrations of polymer are compared.

through independent receptors that converge onto the same intracellular signaling pathways.[17] Moreover, no synergy of polymer action was detected when combinations of active polymers were tested. To further distinguish multivalent structure−activity relationships, we utilized a more flexible polymer backbone with longer interligand spacing and tested the effect on the induction of mouse sperm AE.

AE induction was measured at 5, 10, and 20 μM polymers using a triple-stain flow cytometry assay.[1] Figure 2 illustrates the AE induction efficacy of polycyclooctene and polynorbornene displaying fucose, GlcNAc, or mannose normalized to the positive control of AE induction by calcium ionophore A23187. Polymers displaying glucose were used as a negative control.

In previous work, we observed that for fucose polymers, the level of poly(**1a**)$_{100}$ AE induction increased as the polymer concentration increased from 0.25 to 10 μM with an EC_{50} of 1.6 μM. At higher concentrations of poly(**1a**)$_{100}$, highly cooperative inhibition occurred and the level of AE induction dropped to ∼27%.[1,17] This type of cooperative inhibition is diagnostic of a multivalent activation process that competes poorly with a second monovalent binding event at high probe concentrations.[27−30] Steric occlusion of the cell surface as more receptors are occupied may also prevent di- or multivalent engagement. Mannose and GlcNAc polymers poly(**1b**)$_{100}$ and poly(**1c**)$_{100}$ exhibited similar AE induction plateaus with EC_{50} values of 1.2 and 3.4 μM, respectively. Cooperative inhibition was absent for the mannose polymer and incomplete for the GlcNAc polymer within the testable concentration range.[1,17]

When these same sugar ligands were displayed on polycyclooctene through the same linker, the AE induction profile was distinct from that of the polynorbornene display. The level of AE induction declined for fucose and GlcNAc cyclooctene backbone polymers. Poly(**2a**)$_{100}$ induced <20% AE at 5 μM. Although the level of AE induction continued to increase at higher polymer concentrations, the maximal level of AE induction reached was ∼40%, which was significantly lower than the 100% AE induction observed with poly(**1a**)$_{100}$. The increases were not statistically significant and represent an at

DOI: 10.1021/acs.biochem.7b00166
Biochemistry 2017, 56, 2779−2786

least 10-fold increase in EC_{50} compared to that of the polynorbornene scaffold. Polymers were not tested above 20 μM as sperm viability was reduced upon addition of high polymer concentrations.

The polycyclooctene displaying GlcNAC followed a similar trend. The level of AE induced by poly(**2c**)$_{100}$ increased when the polymer concentration increased from 5 to 20 μM but was not highly statistically significant. Moreover, the maximal level of AE induction observed with poly(**2c**)$_{100}$ was approximately 20%, which is significantly lower than the 100% AE induction by poly(**1c**)$_{100}$.[1] Thus, the EC_{50} is projected to be at least an order of magnitude higher for the polycyclooctene backbone bearing GlcNAc.

In contrast, the level of induction of AE by mannose cyclooctene polymers exceeded 100% at high concentrations. Although both poly(**1b**)$_{100}$ and poly(**2b**)$_{100}$ displayed strong AE induction, poly(**1b**)$_{100}$ induced an AE plateau of 70−80% from 0.25 to 20 μM polymer with an EC_{50} of 1.2 μM;[1] on the other hand, poly(**2b**)$_{100}$ barely induced AE at 5 μM, and the level of induction increased dramatically with an increase in polymer concentration to 10 μM and remained at a plateau up to 20 μM. Thus, the potency of AE induction by polynorbornene polymers ranged from 5- to >10-fold higher than that by polycyclooctene polymers bearing the same sugar. However, the extent of activation was greatest for the polycyclooctene mannose polymer.

Analysis of Glycopolymer Solution Structures. We synthesized polycyclooctenes, poly(**2**)$_{100}$, to form polymers with longer and more flexible backbones compared to the norbornene backbone used initially. We expected that an enhancement of AE activation would be observed because of greater receptor accessibility.[12,13] However, the flexible backbone in combination with fucose or GlcNAc displays a reduced level of AE induction. Only the level of AE induction by mannose polymers increased with the use of polycyclooctene. Therefore, we undertook SAXS analysis of the solution polymer conformations to understand the divergent activities of these polymers.

SAXS measurements were taken on 1 wt % solutions of glycopolymers in M16 medium, the same cell medium used for AE induction but without BSA, which is itself a macromolecule that will scatter X-rays. Spectra were also recorded for the M16 medium without BSA, and this was used as the background signal and subtracted from the data. To eliminate possible artifacts in fitting parameters from the beamstop in the low-q range and points with large uncertainties due to weak signal in the high-q range, SAXS analysis was performed over a q range of approximately 0.01−0.25 Å^{-1}. Although this q range is limited, the data still provide some information about the glycopolymer chain conformation as described further below, yielding insight into possible mechanisms for the observed biological activity.

Figures 3 and 4 show SAXS data for the glycopolymers with polynorbornene and polycyclooctene backbones, respectively. The two data sets display a qualitatively different dependence on q, suggesting different conformations of the glycopolymers with the two different backbones. Analysis of the data in the mid-q range (Figure S1) yields a power law dependence of the scattered intensity on q with an exponent close to −1 in the case of glycopolymers with the norbornene backbones (Table S1), whereas exponents in the range from −1.8 to −3 were found for the glycopolymers with the cyclooctene backbones, with the exception of the polycyclooctene mannose polymer,

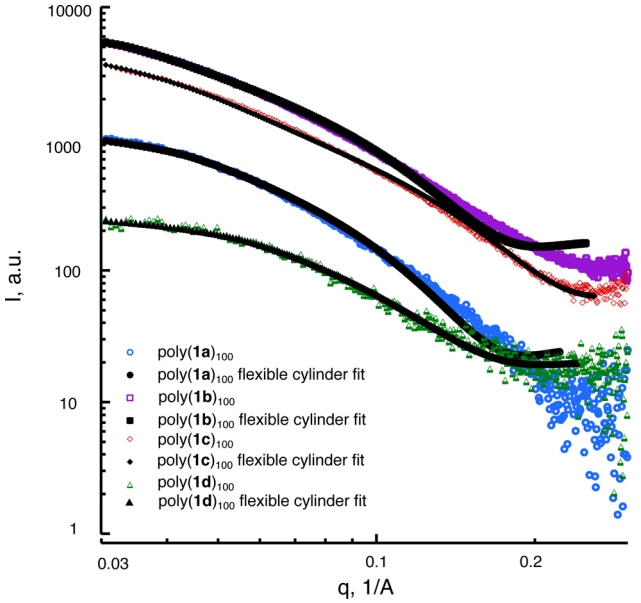

Figure 3. SAXS data for glycopolymers with polynorbornene backbones and fits to flexible cylinder model. Solid lines represent fits to the data.

which displayed an exponent closer to −4, as discussed further below. This suggests a rodlike conformation for the norbornene backbone polymers in solution, while the cyclooctene polymers have a conformation more similar to that of typical flexible polymers in theta to poor solvents, or perhaps a collapsed spherelike structure for the cyclooctene mannose polymer. Thus, an initial analysis of the mid-q range suggested that the same sugar ligands linked to different polymer backbones access distinct solution structures.

A more detailed analysis of data was conducted for both glycopolymers. On the basis of the initial slope value analysis, the norbornene backbone polymers were fit to the flexible cylinder model.[31,32] This model includes contour length L and radius R of a chain comprised of a series of locally stiff segments of length l_p, where $2l_p$ is the Kuhn length. The results are summarized Table 2. The polymers with a norbornene backbone all had similar structures with a contour length in the range of 70−220 Å, a radius of 14−20 Å, and a Kuhn length of 60−100 Å. The Kuhn lengths obtained from data fitting are large, indicating that these polymers are quite rigid (Table 3). Although this result is somewhat unexpected, it is consistent with the findings of Pesek et al., who examined bottlebrush polymers with a norbornene backbone with a length similar to that of our systems, and with polystyrene side chains [PNb(PS)].[33] They performed SANS studies of these polymers in deuterated toluene and attempted to fit the data with a variety of different models. They also found that their systems are described well by the flexible cylinder models and reach contour lengths that are similar to what we find.

COE-backbone polymers, other than poly(**2b**)$_{100}$, were fit to both the flexible cylinder model mentioned above and a model developed for flexible polymer chains with excluded volume interactions, first described by Benoit[34] and later put in analytical form by Hammouda.[35] This model includes the polymer radius of gyration, R_g, and a parameter m that is related to the excluded volume parameter, ν, as $m = 1/\nu$. The results are shown in Figure 4. All polymers show some excess scattering at low q that is not captured by either model, but

DOI: 10.1021/acs.biochem.7b00166
Biochemistry 2017, 56, 2779−2786

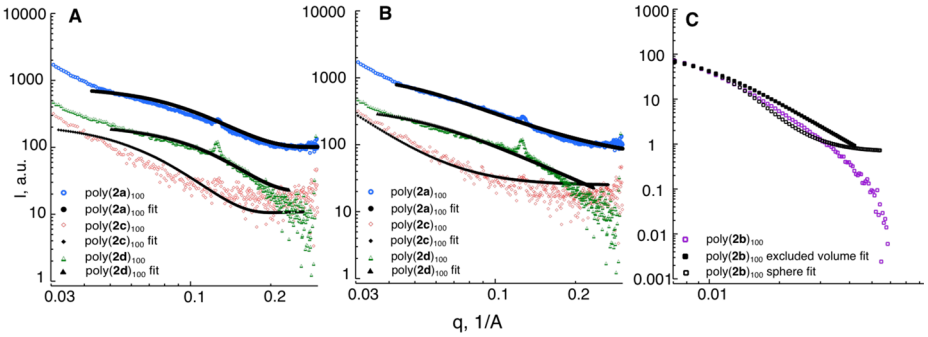

Figure 4. SAXS data for glycopolymers with polycyclooctene backbones. Fits of poly(**2a**)$_{100}$, poly(**2c**)$_{100}$, and poly(**2d**)$_{100}$ to (A) the polymer flexible cylinder model and (B) the excluded volume model. (C) Fits of poly(**2b**)$_{100}$ to the polymer excluded volume model and sphere model.

Table 2. Flexible Cylinder Model Fit Parameters for Poly(NB)s

polymer	contour length (Å)	Kuhn length (Å)	radius (Å)
poly(**1a**)$_{100}$	107.17 ± 0.24	73.06 ± 0.18	19.90 ± 0.02
poly(**1b**)$_{100}$	144.46 ± 0.04	93.11 ± 0.03	18.72 ± 0.003[a]
poly(**1c**)$_{100}$	219.37 ± 0.17	59.82 ± 0.10	14.10 ± 0.01
poly(**1d**)$_{100}$	70.41 ± 0.82	56.64 ± 0.78	18.48 ± 0.08

[a]Uncertainties in fit parameters based on goodness of fit, as provided by the SasView analysis package. Values of <0.01 likely overestimate the true uncertainty and may be due to the limited q range.

because this region is also affected by scattering from the beamstop, it is difficult to discern if this indicates aggregation of chains into larger structures. Accordingly, we focus on fitting data in the mid- to high-q range to obtain information about chain conformation. Fits to the flexible cylinder model for these polymers were performed to facilitate direct comparison of parameters for the two series of polymers; however, the polymer excluded volume model provides a better fit to the data. It is not possible to fit both series of polymers with the polymer excluded volume model, as this model will not reproduce the rigid rod limit.[35]

As shown in Figure 4, spectra from the cyclooctene mannose polymer display behavior qualitatively different from that of other cyclooctene polymers. The mid-q exponent close to −4 displayed by this polymer is impossible to fit with the flexible cylinder model. Although fitting this data with the polymer chain model of Hammouda provides a reasonable fit in the low q range, the excluded volume parameter m reaches the physical limit of 3 for a chain in a poor solvent, the uncertainty in R_g is large, and this model systematically deviates from the data in the mid-q range. Thus, it seems unlikely that the scattering arises from individual chains in a poor solvent. Rather, the shape of the SAXS spectra in the mid-q range is more characteristic of spherical entities. Thus, we show a fit of this data to the form factor for polydisperse spheres. This model provides a better fit to the data in the available q range and reasonable uncertainty in the fit parameters, yielding a radius of ∼78 Å. This polymer did not scatter strongly, and data are available over a limited range of q; thus, we must be cautious in interpreting the SAXS data. Although the different SAXS behavior displayed by this polymer may indicate some type of self-assembly in solution that is not observed in other cyclooctene or norbornene polymers, additional structural information must be obtained before further interpretation.

Results from the fits to the flexible cylinder model for other cyclooctene polymers result in values of L and R that are similar to those of the norbornene polymers (L = 80−170 Å, and R = 14−20 Å), although it should be noted that there is significant uncertainty in the largest value of the contour length. The highest value of L was obtained for the cyclooctene polymer with GlcNAc groups, and data for this sample are noisy. However, all these systems show much smaller values for the Kuhn length, in the range of 7−20 Å, as compared to those of the norbornene backbone polymers. This length is consistent with the cyclooctene backbone polymers having a more flexible structure. Fits to the polymer excluded volume model indicate a radius of gyration of 28−30 Å for the COE polymers with glucose and fucose groups. As expected, the radius of gyration is much smaller than the contour length of the polymer obtained from fits to the flexible cylinder model, again consistent with a much more flexible chain conformation. The value of R_g for the cyclooctene polymer with GlcNAc groups is quite large, 220 Å, although this should be interpreted with caution as there is greater noise in the data for this sample. The values of the parameter m range from 1.8 to 1.9 for the cyclooctene polymers with glucose and fucose groups and to 2.8 for the polymer with GlcNAc groups. We would expect values for parameter m of 1.67 for flexible polymer chains swollen by a good solvent, 2 for chains in a theta solvent, and close to 3 for chains that are collapsed in a poor solvent. The results indicate that the cyclooctene polymers with glucose and fucose groups are

Table 3. Flexible Cylinder or Sphere and Excluded Volume Model Fits of Poly(COE)s

polymer	contour length[a] (Å)	Kuhn length[a] (Å)	radius[a] (Å)	m[b]	R_g[b] (Å)
poly(**2a**)$_{100}$	78.60 ± 3.22	19.65 ± 0.03	13.53 ± 0.03	1.94 ± 0.005[c]	30.69 ± 0.06
poly(**2b**)$_{100}$	–	–	77.64 ± 0.80	3.00[c]	195 ± 3
poly(**2c**)$_{100}$	168.69 ± 47.14	20.00 ± 0.07	18.91 ± 0.30	2.85 ± 0.001[c]	222.08 ± 0.03
poly(**2d**)$_{100}$	97.60 ± 5.59	6.83 ± 0.06	13.99 ± 0.10	1.80 ± 0.02	28.27 ± 0.11

[a]Parameters for flexible cylinder models or, for poly(**2b**)$_{100}$, the polydisperse sphere model. [b]Parameters for excluded volume models. [c]Uncertainties in fit parameters based on goodness of fit, as provided by the SasView analysis package. Values of <0.01 likely overestimate the true uncertainty and may be due to the limited q range. No error is reported for m for poly(**2b**)$_{100}$ as maximal allowable value was reached for this parameter.

DOI: 10.1021/acs.biochem.7b00166
Biochemistry 2017, 56, 2779−2786

behaving as if in a moderately good to theta solvent, with a conformation that is close to an ideal random walk (Figure 5). However, the cyclooctene polymer with GlcNAc groups appears to have a more compact, collapsed configuration.

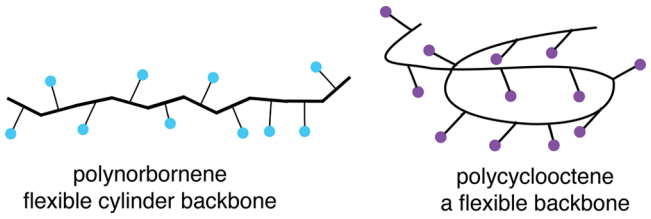

Figure 5. Comparison of polynorbornene and polycyclooctene glycopolymers: (left) polymer with a flexible cylinder backbone and (right) polymer with a flexible random walk backbone.

Earlier studies of polynorbornene backbone conformations focused on characterization of polymers on a surface or in the molten state. The chain conformations exhibited high degrees of heterogeneity. For example, the diblock copolymer of norbornene and organometallic derivatives of norbornene or polyacetylene exhibited different conformations in the film state, including spherical, cylindrical, or lamellar morphology, depending on the diblock compositions and molecular weights. For norbornene backbone brush copolymers containing polylactide (PLA) and poly(*n*-butyl acrylate) (PnBA) side chains, the polymer assembled in a highly ordered lamellar state, with an extended backbone conformation.[36−38] These results provide an estimate of the single-molecule size but do not provide information about their solution-state structures. We conclude that the sugars on our polymers serve to block aggregation of norbornyl chains and help to maintain a flexible cylinder conformation in solution. These structures are analogous to the bottlebrush polymers of Pesek et al.[33] in which the brushes serve to prevent aggregation, where with increase in the length of brushes the conformation underwent a transition from spherical particles to cylinders.

Glycoconjugate conformations have been investigated by SAXS analysis for maltpentaose-carrying polystyrene (PVM5A) and PVLA with PT in water.[39,40] These glycopolymers are often found to self-assemble into nanoparticles, micelles, vesicles, or tubular aggregates because of the amphiphilic nature of the polymers.[41] All of these polymers have flexible backbones, analogous to our polycyclooctene glycopolymers.

CONCLUSION

A series of glycopolymers based on a polycyclooctene backbone was synthesized. These glycopolymers were compared to previously prepared polynorbornene glycopolymers as inducers of mouse sperm acrosomal exocytosis. Per SAXS analyses, the glycopolymers with polynorbornene backbones form flexible cylinders in cell medium. However, glycopolymers with polycyclooctene backbones are significantly less rigid and have conformations typical of polymer chains in a theta to poor solvent. The cylinder conformations are required for efficient acrosomal exocytosis induction by fucose and GlcNAc polymers. Moreover, the proposed spherical conformation adopted by polycyclooctene enhanced mannose induction of AE. Thus, the appropriate choice of polymer backbone for optimal cellular activation is dependent on the sugar displayed. Our results suggest that the AE efficacy of fucose, GlcNAc, and mannose polymers relies on a relatively rigid polymer that can stabilize receptor signaling complexes.

ASSOCIATED CONTENT

Supporting Information

The Supporting Information is available free of charge on the ACS Publications website at DOI: 10.1021/acs.biochem.7b00166.

Supplementary figures, table, and spectra (PDF)

AUTHOR INFORMATION

Corresponding Author

*Department of Chemistry, Stony Brook University, Stony Brook, NY 11794-3400. E-mail: nicole.sampson@stonybrook.edu. Phone: +1-631-632-7952.

ORCID

Nicole S. Sampson: 0000-0002-2835-7760

Funding

This work was supported by National Institutes of Health Grant R01GM097971 (N.S.S.).

Notes

The authors declare no competing financial interest.

ACKNOWLEDGMENTS

The SAXS experiments used resources of the Center for Functional Nanomaterials, a U.S. Department of Energy Office of Science Facility at Brookhaven National Laboratory, under Contract DE-SC0012704, and benefitted from SasView software, originally developed by the DANSE project under National Science Foundation Grant DMR-0520547. We thank Guofang Li for collecting some of the SAXS data.

REFERENCES

(1) Rodolis, M. T., Huang, H., and Sampson, N. S. (2016) Glycopolymer induction of mouse sperm acrosomal exocytosis shows highly cooperative self-antagonism. *Biochem. Biophys. Res. Commun. 474*, 435−440.

(2) Schröter, S., Osterhoff, C., McArdle, W., and Ivell, R. (1999) The glycocalyx of the sperm surface. *Hum. Reprod. Update 5*, 302−313.

(3) Pang, P., Chiu, P. C. N., Lee, C., Chang, L., Panico, M., Morris, H. R., Haslam, S. M., Khoo, K., Clark, G. F., Yeung, W. S. B., and Dell, A. (2011) Human sperm binding is mediated by the sialyl-Lewis(x) oligosaccharide on the zona pellucida. *Science 333*, 1761−1764.

(4) Florman, H. M., and Wassarman, P. M. (1985) O-Linked oligosaccharides of mouse egg ZP3 account for its sperm receptor activity. *Cell 41*, 313−324.

(5) Genbacev, O. D., Prakobphol, A., Foulk, R. A., Krtolica, A. R., Ilic, D., Singer, M. S., Yang, Z., Kiessling, L. L., Rosen, S. D., and Fisher, S. J. (2003) Trophoblast L-selectin mediated adhesion at the maternal-fetal interface. *Science 299*, 405−408.

(6) Kwon, D. S., Gregorio, G., Bitton, N., Hendrickson, W. A., and Littman, D. R. (2002) DC-SIGN-mediated internalization of HIV is required for trans-enhancement of T cell infection. *Immunity 16*, 135−144.

(7) Rabinovich, G. A., van Kooyk, Y., and Cobb, B. A. (2012) Glycobiology of immune responses. *Ann. N. Y. Acad. Sci. 1253*, 1−15.

(8) van Kooyk, Y., and Rabinovich, G. A. (2008) Protein-glycan interactions in the control of innate and adaptive immune responses. *Nat. Immunol. 9*, 593−601.

(9) Lichtenstein, R. G., and Rabinovich, G. A. (2013) Glycobiology of cell death: when glycans and lectins govern cell fate. *Cell Death Differ. 20*, 976−986.

(10) Kiessling, L. L., and Grim, J. C. (2013) Glycopolymer probes of signal transduction. *Chem. Soc. Rev. 42*, 4476−4491.

DOI: 10.1021/acs.biochem.7b00166
Biochemistry 2017, 56, 2779−2786

(11) Choi, S. (2004) *Synthetic multivalent molecules: concepts and biomedical applications*, Wiley, New York.
(12) Kiessling, L. L., Strong, L. E., and Gestwicki, J. E. (2000) Principles for multivalent ligand design. *Annu. Rep. Med. Chem. 35*, 321−330.
(13) Hasegawa, T., Kondoh, S., Matsuura, K., and Kobayashi, K. (1999) Rigid helical poly(glycosyl phenyl isocyanide)s: synthesis, conformational analysis, and recognition by lectins. *Macromolecules 32*, 6595−6603.
(14) Hoshino, Y., Nakamoto, M., and Miura, Y. (2012) Control of protein-binding kinetics on synthetic polymer nanoparticles by tuning flexibility and inducing conformation changes of polymer chains. *J. Am. Chem. Soc. 134*, 15209−15212.
(15) Kanai, M., Mortell, K. H., and Kiessling, L. L. (1997) Varying the size of multivalent ligands: the dependence of concanavalin A binding on neoglycopolymer length. *J. Am. Chem. Soc. 119*, 9931−9932.
(16) Wassarman, P. M. (1999) Mammalian Fertilization: molecular aspects of gamete adhesion, exocytosis, and fusion. *Cell 96*, 175−183.
(17) Wu, L., and Sampson, N. S. (2014) Fucose, mannose, and beta-N-acetylglucosamine glycopolymers initiate the mouse sperm acrosome reaction through convergent signaling pathways. *ACS Chem. Biol. 9*, 468−475.
(18) Loeser, C. R., and Tulsiani, D. R. P. (1999) The role of carbohydrate in the induction of the acrosome reaction in mouse spermatozoa. *Biol. Reprod. 60*, 94−101.
(19) Bielawski, C. W., and Grubbs, R. H. (2007) Living ring-opening metathesis polymerization. *Prog. Polym. Sci. 32*, 1−29.
(20) Lee, Y., and Sampson, N. S. (2006) Romping the cellular landscape: linear scaffolds for molecular recognition. *Curr. Opin. Struct. Biol. 16*, 544−550.
(21) Hillmyer, M. A., Laredo, W. R., and Grubbs, R. H. (1995) Ring-opening metathesis polymerization of functionalized cyclooctenes by a ruthenium-based metathesis catalyst. *Macromolecules 28*, 6311−6316.
(22) Zhang, J., Matta, M. E., and Hillmyer, M. A. (2012) Synthesis of sequence-specific vinyl copolymers by regioselective ROMP of multiply substituted cyclooctenes. *ACS Macro Lett. 1*, 1383−1387.
(23) Love, J. A., Morgan, J. P., Trnka, T. M., and Grubbs, R. H. (2002) A practical and highly active ruthenimu- based catalyst that effects the cross metathesis of acrylonitrile. *Angew. Chem., Int. Ed. 41*, 4035−4036.
(24) Ashby, E. C., and Coleman, D. (1987) Evidence for single electron transfer in the reactions of lithium dimethylcuprate with alkyl halides. *J. Org. Chem. 52*, 4554−4565.
(25) Hartley, D. (1962) Preparation of δ-Oxoaxelaic acid. *J. Chem. Soc.*, 4722−4723.
(26) R Core Team (2017) *R, A Language and Environment for Statistical Computing*, R Foundation for Statistical Computing, Vienna.
(27) Whitty, A., and Borysenko, C. W. (1999) Small molecule cytokine mimetics. *Chem. Biol. 6*, R107−118.
(28) Mack, E. T., Perez-Castillejos, R., Suo, Z., and Whitesides, G. M. (2008) Exact analysis of ligand-induced dimerization of monomeric receptors. *Anal. Chem. 80*, 5550−5555.
(29) Fegan, A., White, B., Carlson, J. C. T., and Wagner, C. R. (2010) Chemically Controlled Protein Assembly: Techniques and Applications. *Chem. Rev. 110*, 3315−3336.
(30) Monine, M. I., Posner, R. G., Savage, P. B., Faeder, J. R., and Hlavacek, W. S. (2010) Modeling multivalent ligand-receptor interactions with steric constraints on configurations of cell-surface receptor aggregates. *Biophys. J. 98*, 48−56.
(31) Pedersen, J. S., and Schurtenberger, P. (1996) Scattering functions of semiflexible polymers with and without excluded volume effects. *Macromolecules 29*, 7602−7612.
(32) Chen, W., Butler, P. D., and Magid, L. J. (2006) Incorporating Intermicellar Interactions in the fitting of SANS data from cationic wormlike micelles. *Langmuir 22*, 6539−6548.
(33) Pesek, S. L., Li, X., Hammouda, B., Hong, K., and Verduzco, R. (2013) Small-angle neutron scattering analysis of bottlebrush polymers prepared via grafting-through polymerization. *Macromolecules 46*, 6998−7005.
(34) Benoit, H. (1957) La diffusion de la lumière par des macromolécules en chaînes en solution en un bon solvant. *Comptes Rendus 245*, 2244−2247.
(35) Hammouda, B. (1993) SANS from homogeneous polymer mixtures - a unified overview. *Adv. Polym. Sci. 106*, 87−133.
(36) Sankaran, V., Cohen, R. E., Cummins, C. C., and Schrock, R. R. (1991) Morphology of diblock copolymers of norbornene and organometallic derivatives of norbornene. *Macromolecules 24*, 6664−6669.
(37) Saunders, R. S., Cohen, R. E., and Schrock, R. R. (1991) Synthesis and characterization of diblock copolymer films containing self-assembled polyacetylene structures. *Macromolecules 24*, 5599−5605.
(38) Xia, Y., Olsen, B. D., Kornfield, J. A., and Grubbs, R. H. (2009) Efficient synthesis of narrowly dispersed brush copolymers and study of their assemblies: the importance of side chain arrangement. *J. Am. Chem. Soc. 131*, 18525−18532.
(39) Wataoka, I., Urakawa, H., Kobayashi, K., Akaike, T., Schmidt, M., and Kajiwara, K. (1999) Structural characterization of glycoconjugate polystyrene in aqueous solution. *Macromolecules 32*, 1816−1821.
(40) Fukuda, T., Inoue, Y., Koga, T., Matsuoka, M., and Miura, Y. (2011) Encapsulation of polythiophene by glycopolymer for water-soluble nanowire. *Chem. Lett. 40*, 864−866.
(41) Delbianco, M., Bharate, P., Varela-Aramburu, S., and Seeberger, P. H. (2016) Carbohydrates in supramolecular chemistry. *Chem. Rev. 116*, 1693−1752.

DOI: 10.1021/acs.biochem.7b00166
Biochemistry 2017, 56, 2779−2786